

# Identifying Electronic Properties Relevant to Improving Stability in a-Si:H-Based Cells and Overall Performance in a-Si,Ge:H-Based Cells

**Annual Subcontract Report,  
18 April 1995 - 17 April 1996**

J.D. Cohen  
*University of Oregon  
Eugene, Oregon*

NREL technical monitor: B. von Roedern



National Renewable Energy Laboratory  
1617 Cole Boulevard  
Golden, Colorado 80401-3393  
A national laboratory of  
the U.S. Department of Energy  
Managed by Midwest Research Institute  
for the U.S. Department of Energy  
under Contract No. DE-AC36-83CH10093

Prepared under Subcontract No. XAN-4-13318-07

March 1997

This publication was reproduced from the best available camera-ready copy submitted by the subcontractor and received no editorial review at NREL.

### **NOTICE**

This report was prepared as an account of work sponsored by an agency of the United States government. Neither the United States government nor any agency thereof, nor any of their employees, makes any warranty, express or implied, or assumes any legal liability or responsibility for the accuracy, completeness, or usefulness of any information, apparatus, product, or process disclosed, or represents that its use would not infringe privately owned rights. Reference herein to any specific commercial product, process, or service by trade name, trademark, manufacturer, or otherwise does not necessarily constitute or imply its endorsement, recommendation, or favoring by the United States government or any agency thereof. The views and opinions of authors expressed herein do not necessarily state or reflect those of the United States government or any agency thereof.

Available to DOE and DOE contractors from:  
Office of Scientific and Technical Information (OSTI)  
P.O. Box 62  
Oak Ridge, TN 37831  
Prices available by calling (423) 576-8401

Available to the public from:  
National Technical Information Service (NTIS)  
U.S. Department of Commerce  
5285 Port Royal Road  
Springfield, VA 22161  
(703) 487-4650



## PREFACE

This Annual Technical Progress Report covers the work performed at the University of Oregon for the period 18 April 1995 to 17 April 1996 under NREL Subcontract Number XAN-4-13318-07. The following personnel participated in this research program:

NAME	TITLE	WORK PERFORMED
J. David Cohen	Principal Investigator	Program Manager
C. Palsule	Research Associate	Characterization of the hetero-junction interface between a-Si:H and a-Si,Ge:H Alloys
Daewon Kwon	Research Assistant	Stability Studies of H-diluted a-Si:H samples
Chih-Chiang Chen	Research Assistant	Characterization of the stability of a-Si,Ge:H Alloys

## TABLE OF CONTENTS

	Page
<b>LIST OF ILLUSTRATIONS</b> .....	iii
<b>LIST OF TABLES</b> .....	iv
<b>EXECUTIVE SUMMARY</b> .....	v
<b>1.0 INTRODUCTION</b> .....	1
<b>2.0 SAMPLES</b>	
2.1 GLOW DISCHARGE AMORPHOUS SILICON- GERMANIUM ALLOYS.....	1
2.2 AMORPHOUS SILICON/AMORPHOUS SILICON-GERMANIUM HETEROJUNCTION SAMPLES.....	2
2.3 HYDROGEN AND HELIUM DILUTED AMORPHOUS SILICON .....	3
<b>3.0 EXPERIMENTAL CHARACTERIZATION METHODS</b>	
3.1 ADMITTANCE SPECTROSCOPY .....	5
3.2 DRIVE-LEVEL CAPACITANCE PROFILING .....	5
3.3 TRANSIENT CAPACITANCE SPECTROSCOPY .....	6
3.3 TRANSIENT PHOTOCAPACITANCE AND PHOTOCURRENT.....	7
<b>4.0 DEGRADATION OF AMORPHOUS SILICON-GERMANIUM ALLOYS.</b>	8
<b>5.0 ELECTRONIC PROPERTIES OF THE a-Si:H/a-Si<sub>x</sub>Ge<sub>1-x</sub>:H HETEROJUNCTION INTERFACE</b> .....	11
<b>6.0 PROPERTIES OF a-Si:H DEPOSITED WITH HYDROGEN OR HELIUM DILUTION</b> .....	17
<b>7.0 SUMMARY AND CONCLUSIONS</b> .....	20
<b>8.0 SUBCONTRACT SUPPORTED PUBLICATIONS</b> .....	21
<b>9.0 REFERENCES</b> .....	22

## LIST OF ILLUSTRATIONS

	Page
FIG. 1. Schematic diagram indicating basic sequence of events in semiconducting junction transient measurements.....	6
FIG. 2 Example of drive-level profiling measurements for one a-Si,Ge:H alloy sample in its dark annealed state .....	8
FIG. 3. Summary of drive-level densities vs. emission energy for three a-Si,Ge:H samples .....	9
FIG. 4. Transient photocapacitance and photocurrent spectra for the annealed and light soaked state of one 35at.% Ge sample.....	10
FIG. 5. Densities of states employed to fit sub-band-gap optical spectra of Fig. 4.....	10
FIG. 6. Comparison of deep defect densities obtained for seven a-Si,Ge:H samples obtained from capacitance profiling and sub-band-gap spectra .....	11
FIG. 7. Capacitance vs. time following a 300s long voltage filling pulse for one a-Si:H/a-Si,Ge:H heterojunction sample.....	12
FIG. 8. Capacitance overshoot vs. the product of the filling pulse voltage and the filling pulse duration for heterojunction sample 6 .....	13
FIG. 9. Capacitance transients for heterojunction sample 7 using different ambient bias voltages .....	15
FIG. 10. Charge transients deduced from capacitance transient measurements on a-Si:H/a-Si,Ge:H heterojunction samples .....	15
FIG. 11. Example of drive-level capacitance profiling data for hydrogen diluted a-Si:H sample .....	18
FIG. 12. Comparison of drive-level densities for different contacting configurations for two types of a-Si:H films .....	18
FIG. 13. Comparison of drive-level determined defect densities for one hydrogen diluted and an undiluted sample vs. light exposure .....	19

**LIST OF TABLES**

<b>TABLE I.</b>	Summary of sample configurations for a-Si:H/a-Si,Ge:H heterojunction samples.....	3
<b>TABLE II.</b>	Deposition conditions for the i-layers of a-Si:H samples produced at Lawrence Berkeley Laboratory .....	4
<b>TABLE III.</b>	Summary of deduced interface trap densities for a-Si:H/a-Si,Ge:H heterojunction samples.....	16
<b>TABLE IV.</b>	Carrier mobilities and deep defect densities for LBL a-Si:H samples in their dark annealed states .....	19

## EXECUTIVE SUMMARY

The work carried out during this second phase of our NREL Subcontract has been focused on degradation studies in both pure a-Si:H and the a-Si,Ge:H alloys, as well as a detailed study of the interface between these two materials in a-Si:H/a-Si,Ge:H heterostructures. All samples discussed in this report were produced by the glow discharge method. They were obtained either in collaboration with United Solar Systems Corporation or with researchers at Lawrence Berkeley Laboratory.

First, the results from our a-Si,Ge:H degradation studies support the conclusion that there exist considerable quantities of charged defects in nominally intrinsic material. We found that, upon light soaking all the observed defect sub-bands increased; however, their ratios varied significantly. This indicates a *change in the ratios* of the defects in the different charge states. This will undoubtedly have important consequences for better understanding the degradation process in a-Si,Ge:H devices.

Second, we performed voltage pulse stimulated capacitance transient measurements on a-Si:H/a-Si,Ge:H heterostructure samples and found a clear signature of trapped hole emission extending over long times. We were able to confirm that these hole traps were associated specifically with the interface itself in concentrations of roughly  $10^{11} \text{ cm}^{-2}$ . We found that treatment or grading of the interface modified the concentrations of these hole traps. However, these traps did not seem to act as recombination centers for electrons brought into the interface region.

Finally, we have begun comparison studies of the electronic properties a-Si:H grown by glow discharge either with 100% silane, or with silane diluted in  $\text{H}_2$  or He gas. These samples were predominantly n-i-p structures deposited on Cr coated glass, thus closely reproducing a popular photovoltaic device geometry. The results on these samples indicate that the films grown under high hydrogen dilution exhibit roughly a factor of three lower deep defect densities than those grown using pure silane. Furthermore, in preliminary studies of light induced degradation, the hydrogen diluted samples degraded at a slower rate and saturated at a level lower by about a factor of five than the pure silane deposited sample.

## 1.0 INTRODUCTION

The work carried out in Phase I under NREL Subcontract XAN-4-13318-07 has concentrated on three types of studies. First, we have examined the degradation of glow discharge a-Si,Ge:H alloy films by observing the increase in deep defect density using both capacitance profiling and sub-band-gap optical spectra. These studies suggest a prominent role for more than a single charge state of the dominant deep defect.

Second, we have carried an extensive evaluation of the electronic properties of the a-Si:H/a-Si,Ge:H heterojunction interface using capacitance transient methods. These measurements have disclosed significant densities of hole traps in the vicinity of this interface. We discuss the possible effects these hole traps could have on the properties of tandem solar cells that incorporate such interfaces between layers of a-Si:H and a-Si,Ge:H.

Finally, we report some ongoing work to compare the stability of glow discharge a-Si:H grown with or without H<sub>2</sub> dilution. Our preliminary results indicate a greatly improved stability of the latter material with regard to light induced defect creation. This correlates well with the reported improved stability of cells fabricated from H<sub>2</sub> diluted material.

In the Sections that follow, we first describe the samples studied and then briefly review the experimental techniques employed. In Section 4 we discuss our results concerning the degradation of the glow discharge a-Si,Ge:H samples. In Section 5 we present our results on the electronic properties of the a-Si:H/a-Si,Ge:H interface, and in Section 6 our results on hydrogen diluted a-Si:H. Finally, in Section 7 we summarize our findings and draw some general detailed conclusions.

## 2.0 SAMPLES AND SAMPLE TREATMENT

### 2.1 GLOW DISCHARGE AMORPHOUS SILICON-GERMANIUM ALLOYS

Seven a-Si,Ge:H films were deposited by the rf glow discharge method at United Solar Systems Corporation (courtesy of J. Yang and S. Guha). These were deposited on heavily p-type doped crystalline Si substrates at 300°C using mixtures of Si<sub>2</sub>H<sub>6</sub> and GeH<sub>4</sub> gases diluted in H<sub>2</sub>. The GeH<sub>4</sub> flow rate was varied to obtain different Ge fractions. Additional details of the deposition conditions have been described elsewhere [1]. The Ge fractions were determined by electron microprobe measurements, courtesy of Harv Mahan and Alice Mason at NREL. Five of the samples studied had Ge fractions in the range 30 to 35at.%, considered the most suitable for the low gap alloy of tandem solar cells. The remaining two samples had Ge fractions near

20at.% and 50at.%, respectively. These samples were included to help identify behavioral trends in the alloy series. To investigate the defect properties by our junction capacitance and photocurrent methods described below, semitransparent Pd contacts were evaporated on each film. However, in all the studies reported for these samples (see Section 4), the contact at the silicon substrate was employed as the active junction.

The a-Si,Ge:H alloy samples were annealed at 460K for one hour before the initial series of measurements (state A). To study the light soaked states these samples were exposed for 70 to 100 hours to a focussed tungsten halogen light source using an appropriate long pass filter to achieve uniform carrier generation rates over the 1 to 2 $\mu$ m thickness of each sample. Measured intensities for light soaking were 6W/cm<sup>2</sup> for the 30-35at.% alloys, 4.5W/cm<sup>2</sup> for the 50at.% alloy, and 6W/cm<sup>2</sup> for the 20at.% alloy. To maintain a low temperature during light exposure each sample was immersed in methanol. This guaranteed a surface temperature below 65°C.

## 2.2 AMORPHOUS SILICON/AMORPHOUS SILICON-GERMANIUM HETERO-JUNCTION SAMPLES

To investigate the electronic properties of the heterojunction between a-Si:H and the a-Si,Ge:H alloys eight samples were also prepared by J. Yang and S. Guha at United Solar Systems Corporation. The substrates were heavily p-type doped crystalline Si and the alloy Ge fraction was 30-35at.% for all samples. All samples consisted of a 1.2-1.5 $\mu$ m a-Si,Ge:H alloy layer together with a 3000-5000Å layer of a-Si:H. For six samples the a-Si:H was deposited first, followed by the a-Si,Ge:H; however, for two samples this order was reversed. In two samples the transition between a-Si:H and a-Si,Ge:H alloy was graded rather than abrupt. And, in one case, the a-Si:H layer was subjected to a special surface treatment before the beginning of a-Si,Ge:H deposition. Table I provides the details of the configurations of the eight samples in this part of our study.

Semitransparent Cr or Pd contacts (area of  $2 \times 10^{-3}$  cm<sup>2</sup>) were evaporated on the top layer of each of these samples to form a Schottky barrier. Thus, the a-Si:H/a-Si,Ge:H interface was positioned within 3000-5000Å of either this Schottky barrier or the substrate junction. This enabled its electronic properties to be probed capacitively. Results of our studies of these samples are presented in Section 5.

**TABLE I.** Summary of configurations for a-Si:H/a-Si,Ge:H heterojunction samples. The interface treatment for Sample 6 is a proprietary process of United Solar Systems.

#	First Layer	Interface	Second layer
1	a-Si:H (3000 Å)	Untreated	a-Si,Ge:H (1.2 μm)
2	a-Si,Ge:H (1.2 μm)	Untreated	a-Si:H (3000 Å)
3	a-Si:H (5000 Å)	Untreated	a-Si,Ge:H (1.2 μm)
4	a-Si,Ge:H (1.2 μm)	Untreated	a-Si:H (5000 Å)
5	a-Si:H (4000 Å)	Untreated	a-Si,Ge:H (1.5 μm)
6	a-Si:H (4000 Å)	Treated	a-Si,Ge:H (1.5 μm)
7	a-Si:H (4000 Å)	Graded (250 Å)	a-Si,Ge:H (1.5 μm)
8	a-Si:H (4000 Å)	Graded (1000 Å)	a-Si,Ge:H (1.5 μm)

### 2.3 HYDROGEN AND HELIUM DILUTED AMORPHOUS SILICON

To investigate reports of improved stability of glow discharge a-Si:H deposited under conditions of silane dilution, we obtained a series of samples from collaborators at Lawrence Berkeley Laboratory (from the group of V. Perez-Mendez). They employed a conventional plasma enhanced CVD reactor employing an rf frequency of 85MHz. One sample was of their standard glow discharge sample material grown with 100% SiH<sub>4</sub>, three samples were grown using mixtures of H<sub>2</sub> and SiH<sub>4</sub> in a ratio of 15-to-1, and two were grown using mixtures of He and SiH<sub>4</sub> in a ratio of 2-to-3. These six films were deposited on substrates of Corning 7059 glass and consisted of a n<sup>+</sup>, intrinsic, and p<sup>+</sup> doped layers. The i-layers were at least 2μm thick. Substrate temperatures were varied between 190°C to 250°C. The top and bottom layers were contacted with sputtered semitransparent Cr. Details of the growth conditions for each of these samples are given in Table II.

In addition to these n-i-p samples, two additional sample configurations were studied. In one case, before deposition of the top Cr contact, the p<sup>+</sup> a-Si:H layer was removed using a SF<sub>6</sub> plasma etch, and then a Pd Schottky contact was deposited directly onto the exposed i-layer. This configuration will be referred to as an n-i-m structure. Also, a purely intrinsic a-Si:H layer

was deposited directly onto a  $p^+$  crystalline Si substrate, followed by the deposition of a Pd Schottky top contact. This will be denoted as the  $p^+(c\text{-Si})\text{-i-m}$  sample.

Defect densities in these samples were determined before and, in a couple cases, after light soaking using drive-level capacitance profiling. Light soaking was carried out using a red filtered tungsten halogen light source at a power level of  $3.4\text{W}/\text{cm}^2$ . Samples were immersed in methanol during light exposure to ensure a low surface temperature (significantly below  $65^\circ\text{C}$ ). The experimental results concerning the stability of these samples with respect to light-induced deep defect creation are presented in Section 6 below.

**TABLE II.** Deposition conditions for the i layers of a-Si:H samples produced at Lawrence Berkeley Laboratory (courtesy of F. Zhong, W.S. Hong, and V. Perez-Mendez).

Sample (Dilutant)	$[\text{H}_2]/[\text{SiH}_4]$ $[\text{He}]/[\text{SiH}_4]$	Temperature ( $^\circ\text{C}$ )	Pressure (mTorr)	Power Density ( $\text{mW}/\text{cm}^2$ )	Dep. Rate ( $\mu\text{m}/\text{hr}$ )	i-layer thickness
1 ( $\text{H}_2$ )	15	190	1000	60	1.4	$5.2\ \mu\text{m}$
2 ( $\text{H}_2$ )	15	190	1000	90	1.5	$6.2\ \mu\text{m}$
3 ( $\text{H}_2$ )	15	250	1000	60	1.1	$4.8\ \mu\text{m}$
4 (He)	0.67	150	500	90	3.5-4	$4.0\ \mu\text{m}$
5 (He)	0.67	250	500	90	3.5-4	$7.8\ \mu\text{m}$
6 (none)	0.00	1.0	300	40	2.3	$10.\ \mu\text{m}$

### 3.0 EXPERIMENTAL CHARACTERIZATION METHODS

The measurements employed in our studies rely on a set of experimental techniques which have all been described previously in some detail. They consist of (1) admittance spectroscopy as a function of temperature and frequency, (2) drive-level capacitance profiling, (3) transient capacitance spectroscopy, and (3) transient photocapacitance taken together with transient junction photocurrent spectroscopy. For the purpose of this report we will describe each method only very briefly and review what kind of information is obtained from each type of measurement.

### 3.1 ADMITTANCE SPECTROSCOPY

Our Schottky diode samples contain a depletion region which is characterized as a function of temperature and frequency before we undertake the more sophisticated capacitance based measurements described in Sections 3.2 to 3.4 below. Such measurements provide us with an estimate of our film thickness (the temperature independent region at low T is simply related to the geometric thickness,  $d$ , by the formula  $C = \epsilon A/d$ ), and an Arrhenius plot of the frequency of the lowest temperature capacitance step (or conductance peak) vs.  $1/T$  provides us with the activation energy of the ac conductivity,  $E_{\sigma}$ , which we identify with the Fermi energy position:  $E_{\sigma} = E_C - E_F$ . [2] These admittance measurements also give us an indication of the quality of our Schottky barriers which allow us to pre-screen our samples for further study.

### 3.2 DRIVE-LEVEL CAPACITANCE PROFILING

The drive-level capacitance profiling method has been described in detail in many publications [3,4]. It is similar to other kinds of capacitance profiling in that it provides us with a density vs. distance profile; however, this particular method was developed specifically to address the difficulties encountered in interpreting capacitance measurements in amorphous semiconductors. In this method we monitor the junction capacitance both as a function of DC bias,  $V_B$ , and as a function of the amplitude of the alternating exciting voltage,  $\delta V$ . One finds that to lowest order this dependence obeys an equation of the form:

$$C(V_B, \delta V) = C_0(V_B) + C_1(V_B) \delta V + \dots$$

and that the ratio

$$N_{DL} \equiv \frac{C_0^3}{2q_e \epsilon A^2 C_1} \quad (1)$$

is directly related to an integral over the density of mobility gap defect states:

$$N_{DL} = \int_{E_c - E_e}^{E_F^0} g(E) dE \quad (2)$$

Here  $E_F^0$  is the bulk Fermi level position in the sample and  $E_e$  depends on the frequency and temperature of measurement:

$$E_e(\omega, T) = k_B T \log(v/\omega) \quad (3)$$

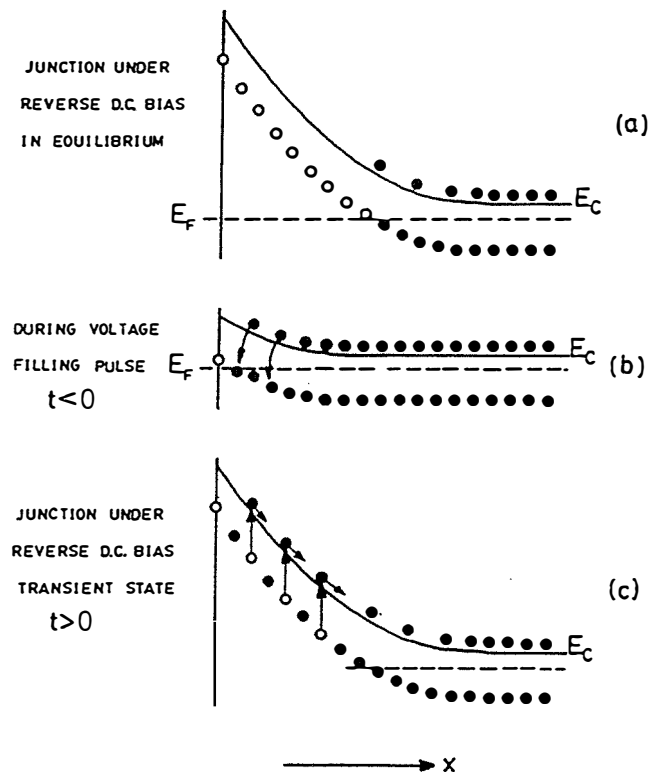
Thus, by altering the measurement temperature (or frequency) we obtain information about the energy distribution of the defects and, by altering the applied DC bias, we can vary the spatial region at which we detect the defects in the sample. That is, we can spatially profile the defects as a function of the position from the barrier interface.

In our current studies we typically measured 10 or 100Hz profiles for a series of temperatures between 320K to 360K. These data usually indicated a clear upper limit for  $N_{DL}$  which, we have shown [5], is equal to roughly one half the total defect density in these samples. This thus provides us with a quantitative measurement of the deep defect levels. In addition, because of the profiling information also obtained, we are able to assess the spatial uniformity of the electronic properties in these samples.

### 3.3 TRANSIENT CAPACITANCE SPECTROSCOPY

The general method of junction transient measurements on amorphous semiconductors has been discussed in detail in several earlier publications.[2,6,7] The basic physics of all such measurements is as shown in Fig. 1. We illustrate the situation for a semiconductor with one discrete deep gap states within the space charge region of a Schottky barrier which is subjected to a voltage "filling pulse". This pulse causes a non-equilibrium (filled) occupation of gap state to be established. As time progresses, the initial steady-state population is recovered through the excitation of trapped electrons to the conduction band where they can then move out of the depletion region under the influence of the electric field. In the dark this process proceeds entirely by the thermal excitation of trapped carriers. However, this process can be enhanced through optical excitation which is the basis of the photocapacitance and junction photocurrent techniques described Section 3.4 below.

**FIG. 1.** Schematic diagram indicating the basic sequence of events in semiconducting junction transient measurements: (a) Junction under reverse bias in quasi-equilibrium showing the electronic occupation of gap states (solid circles) plus empty gap states above  $E_F$  in deep depletion (open circles). (b) During voltage "filling pulse" gap states capture electrons from the conduction band. (c) Reverse bias is restored and occupied gap states above  $E_F$  are slowly released to the conduction band due to thermal or optical excitation processes.



The re-equilibration can be observed by the redistribution of trapped carriers, either as a change in the *junction capacitance* (which occurs because the depletion region will contract as negative charge is lost and the positive charge density increases) or by monitoring the *current* which results from the motion of this charge. However, the observation of capacitance transients has one significant difference compared to current transient measurements: The dominant type of emitted carrier (electron or hole) can be identified by the *sign* of the observed change in capacitance.

### 3.4 TRANSIENT PHOTOCAPACITANCE AND PHOTOCURRENT

The methods of junction transient photocapacitance and photocurrent have been discussed by us in great detail recently in the literature [8,9,10] and also in previous NREL reports. They represent types of sub-band-gap optical spectroscopy and provide spectra quite similar in appearance to PDS derived sub-band-gap optical absorption spectra or to CPM spectra. Instead of detecting absorbed energy, however, our photocapacitance and photocurrent transient methods detect the optically induced change in defect charge within the depletion region. However, unlike the CPM method, both of our junction based techniques are not greatly influenced by the free carrier mobilities since, once an electron (or hole) is optically excited into the conduction (valence) band it will either totally escape the depletion region on the slow timescale of our measurement (0.1 to 1s) or be retrapped into a deep state and not escape. In most cases we assume that almost all of the optically excited majority carriers (electrons) *do* escape but, in general, only a fraction of the minority carriers (holes).

Because the photocapacitance and photocurrent measurements have different sensitivities to the loss of electrons *vs.* holes from the depletion region, a detailed comparison of the two kinds of spectra can be used to disclose the escape length of the holes.[8,11] This allows us to estimate the hole  $\mu\tau$  products for these samples. In these experiments the parameter  $\tau$  is identified as a deep trapping time, *not* a recombination time. We are also able to distinguish whether optical excitation of defect states comes about because of the excitation of trapped electrons to the conduction band or because of the excitation of valence band electrons into an empty mobility gap state. This ability to distinguish electron from hole processes is unique among all the various types of sub-band-gap optical spectroscopies.

#### 4.0 DEGRADATION OF AMORPHOUS SILICON-GERMANIUM ALLOYS

In Figure 2 we display the results of drive-level capacitance profiling measurements for sample 6565 (35at.% Ge) in its annealed states as a function of measurement temperature. These profiles indicate very uniform sample properties, and the profile density is observed to reach a limiting value as the temperature is increased. Figure 3 displays the average DLCP profile values for three of the a-Si,Ge:H samples in their annealed and light-soaked states as a function of temperature expressed as thermal energy depth via Eq. (3). Each of these DLCP measurements indicate a clear upper limit as this energy depth is increased, and this limit represents the total defects in a band of thermal excited transitions we will refer to as TH1. We find very similar defect densities for samples 6286 and 6565 (a 30at.% and 35at.% Ge containing alloy, respectively) in both their dark annealed and light soaked states. The degraded states for these samples indicate a factor of 2 to 2.5 increase in the defect density over the annealed states within the TH1 band. The 50at.% sample shows a much higher defect density for this band in its annealed state, and this density increases by only a factor of 1.4 after light soaking. A summary of the defect densities before and after light soaking in the TH1 defect band for all seven samples is shown in Fig. 6(a).

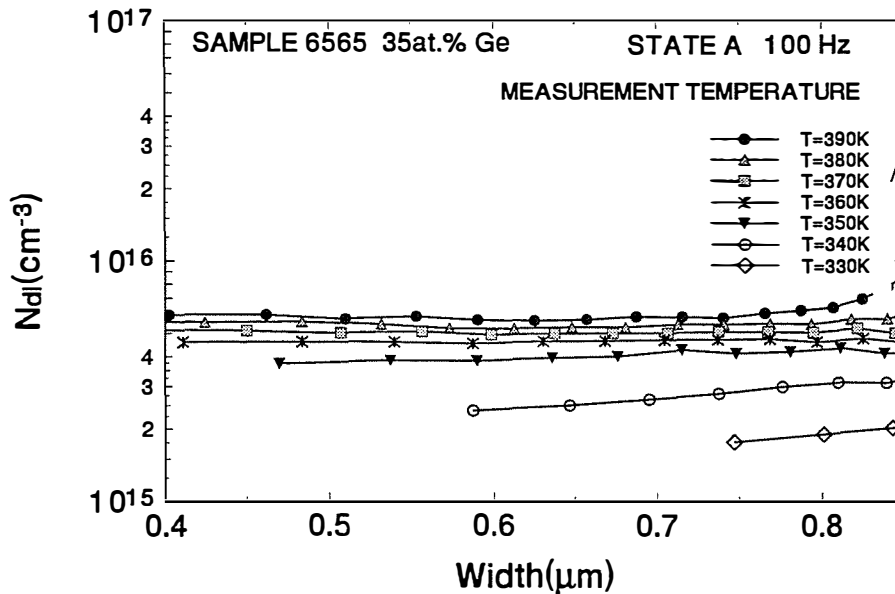


**FIG. 2.** Example of drive-level profiling measurements for one a-Si,Ge:H alloy sample in its dark annealed state. At high temperatures the value of  $N_{d1}$  reaches a limiting value, and it is this value we assign to the deep defect band denoted as TH1.

**FIG. 3.** Summary of drive-level densities vs. emission energy ( $E_e = k_B T \log(v/\omega)$ ) for three a-Si,Ge:H samples: 6286 with 30at.% Ge, 6565 with 35at.%, and 6384 with 50at.% Ge. Closed symbols represent values for the annealed states of each sample, and open symbols the light soaked states. Note that all profiles reach a limiting value as  $E_e$  is increased.

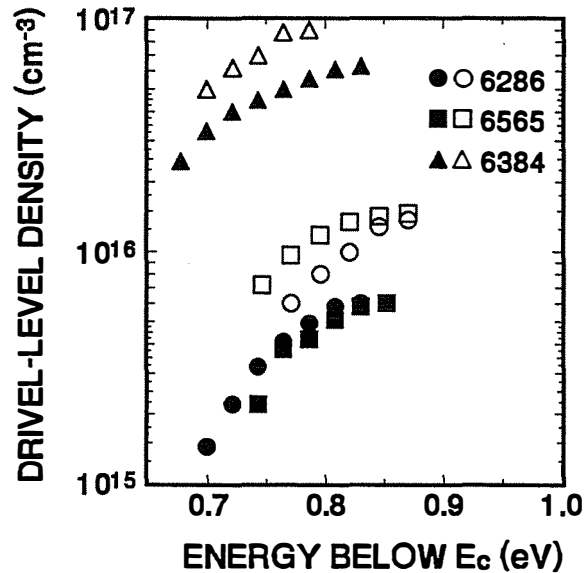


Figure 4 presents two typical transient photocapacitance and photocurrent spectra for samples 6565 (35at.% Ge) in its annealed and light soaked states. Both these pairs of spectra (and those for the other a-Si,Ge:H samples) are fit quite well by a model employing two Gaussian shaped defect sub-bands representing transitions from a defect electron into the conduction band (OP1), and from the valence band into an empty defect level (OP2). A schematic of these transitions used to fit the data of Fig. 4 are given in Fig. 5. The details of this fitting process have been described previously [12,13], and we have also noted that the band of defects, OP2, exhibits a very slow re-emission of the electron optically excited into it from the valence band. On the other hand, modulated photocurrent measurements (MPC) have revealed a band of electron trapping states in these alloy samples [13], from which the electron re-emission occurs very rapidly. Because of this, we know that there must exist significant contributions of at least two distinct defect sub-bands in the a-Si,Ge:H alloys. A reasonable working hypothesis is that the OP2 transition is due to valence band electrons excited into  $D^+$  states, while the MPC signal is due to electron capture into  $D^0$  states. This would be consistent with the observed very different electron re-emission rates, and would account for the observations within the context of a single type of defect.

In Figures 6(b) and 6(c) we have summarized the magnitudes of the defect bands OP1 and OP2 for each of the seven alloy samples studied. We find that for most samples, the magnitudes of each of the deduced defect bands, TH1, OP1, and OP2, increase after light soaking. However, the relative factors of these increases vary among the samples studied. In addition, the TH1 defect densities are slightly higher in the more recently grown 35at.% Ge samples (8257 and 8330) than the earlier samples (6558 and 6565) while the OP2 densities are significantly lower. Also, the recent sample pair exhibit slightly lower conductivity activation

energies (by about 50meV in the annealed state) indicating a slightly greater n-type character to these two samples. This supports the assignment of  $D^+$  to the OP2 defect band. The TH1 and OP1 signals arise from electrons excited out of  $D^-$  states, or  $D^0$  states, or some combination of the two. Since the increase of OP1 and TH1 with light soaking is different among the samples, this suggests that both  $D^-$  and  $D^0$  states are involved. We think it likely that the TH1 determined defect density is more heavily weighted toward  $D^-$  states than is the OP1 defect density.

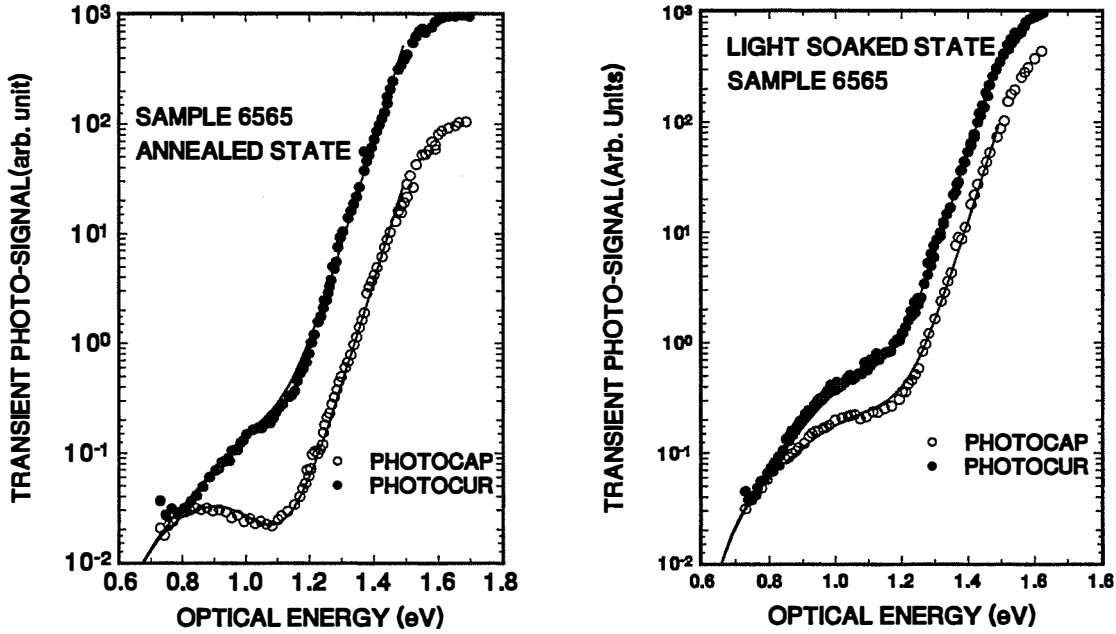
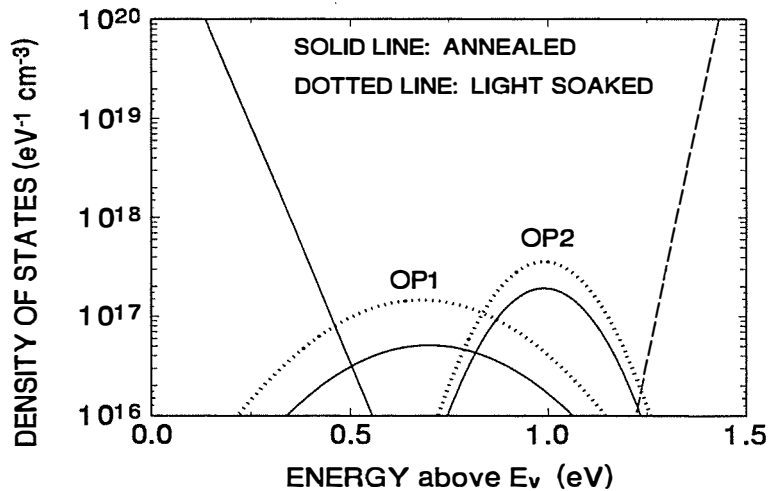
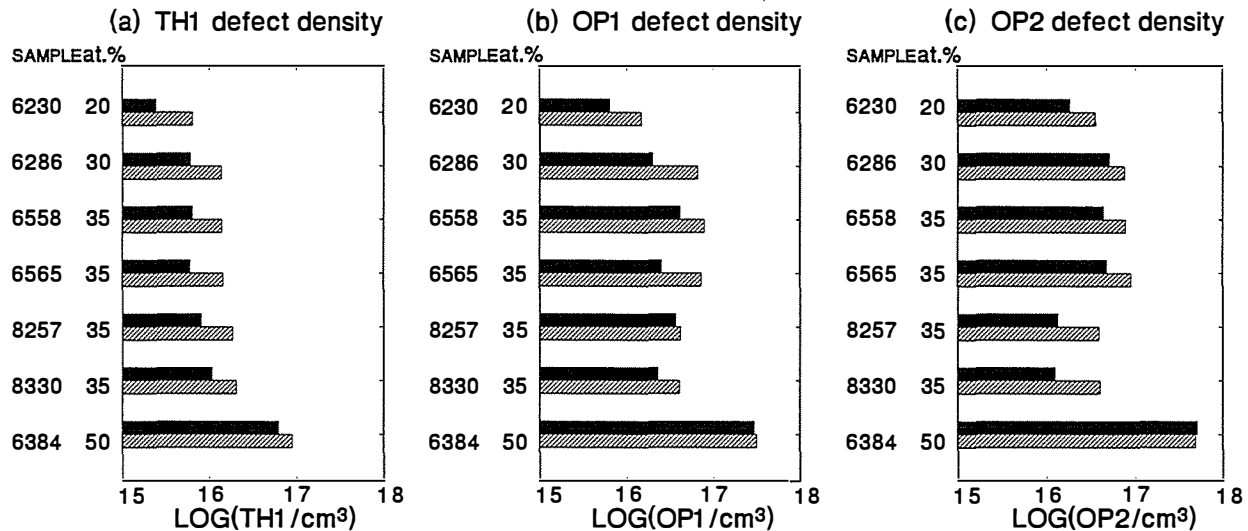


FIG. 4. The transient photocapacitance and photocurrent spectra for the annealed and light soaked state of one 35at.% Ge sample. The solid lines drawn through the data points represent the results of a model calculation incorporating two optical bands for the deep defect transitions: OP1 and OP2, as shown in Fig. 5.

FIG. 5. Densities of states employed to fit sub-band-gap optical spectra of Fig. 4. Light induces transitions *out of* the band labeled OP1 into the conduction band, and induces transitions from the valence band *into* the band labeled OP2. The valence band-tail region is also incorporated into the fitting procedure and thus yields a value for the Urbach energy. The conduction band-tail distribution is not incorporated into the fits and is shown only for illustration.





**FIG. 6.** Comparison of the deep defect densities obtained for seven a-Si,Ge:H samples obtained from capacitance profiling (TH1), and from sub-band-gap optical spectra (OP1 and OP2) in both the dark annealed (solid bars) and light soaked states (shaded bars). The variation between TH1, OP1, and OP2 indicates that more than a single defect sub-band must be involved. We believe the OP2 band arises from  $D^+$  states, while the TH1 and OP1 bands arise from  $D^-$  and/or  $D^0$  states.

The inferred presence of charged defect states in the a-Si,Ge:H alloys, and the fact that their ratios appear to change as a result of light soaking, is clearly very important regarding light induced degradation of photovoltaic devices fabricated from these alloys. Indeed, modeling of a-Si,Ge:H p-i-n cells based only upon the observed increase in deep defects after light soaking (in companion films) have failed to account for the observed changes in device performance.[14] Because our experimental results indicate that there exist significant concentrations of charged defects even in the most intrinsic a-Si,Ge:H alloys, these definitely need to be included in future device modeling studies. This is to be contrasted to the case of pure a-Si:H where device modeling has produced more reasonable results. Indeed, our experimental results for intrinsic a-Si:H do *not* require the presence of more than a single charge state ( $D^0$ ) of the dominant defect. Our plans for the near future regarding studies of a-Si,Ge:H include obtaining very lightly doped n and p-type samples so that we can more quantitatively determine the concentrations of deep defects in their different charge states.

## 5.0 ELECTRONIC PROPERTIES OF THE a-Si:H/a-Si,Ge:H HETEROSTRUCTURE INTERFACE

Amorphous silicon (a-Si:H) based multi-junction photovoltaic devices incorporate silicon-germanium alloys (a-Si,Ge:H) for the bottom and/or middle cell. [1,2] It is therefore

quite likely that the properties of the a-Si:H/a-Si,Ge:H interface play a key role in determining the performance and the stability of an individual p-i-n cell.[4] In this Section we present results from capacitance transient measurements which disclose a significant concentration of hole traps at this interface. Since hole transport in a-Si:H based solar cells is the limiting factor [3], these results may be quite significant.

The sample configuration used for these measurements have been given in Section 2. A total of eight samples were studied consisting of a thinner (3000-5000Å) layer of a-Si:H next to a thicker layer of a-Si,Ge:H alloy with roughly 35at.% Ge. The opposite side of the a-Si:H layer was contacted either with a heavily doped p+ crystalline Si substrate or a metal Schottky barrier. Thus, the resulting a-Si:H/a-Si,Ge:H heterojunction was positioned within 3000-5000Å of either the Schottky barrier or substrate junction so that its electronic properties could be probed capacitively. The capacitance transient measurements described below were carried out at a temperature of 370K.

We applied a filling pulse to place the junction nearest to the a-Si:H/a-Si,Ge:H interface into forward bias and then recorded the capacitance transients after restoring the initial reverse bias. Under these pulsing conditions all the samples, except those in which the interface was adjacent to the Schottky barrier (i.e., samples 2 and 4), exhibited a particular type of capacitance transient. As displayed in Fig. 7, the transients can be divided into two time regimes: a short time regime, in which the capacitance increases with time corresponding to a *loss* of negative charge (electron-emission type), and a long time regime, in which the capacitance decreases with time corresponding to a *gain* of negative charge (hole-emission type). If the filling pulse voltage

**FIG. 7.** Capacitance vs. time following a 300s long voltage filling pulse to +0.28 volts (solid circles) or to zero volts (solid triangles). The ambient bias was -3V. The four transients denoted with open symbols were again obtained using a 300s filling pulse to +0.28 volts, but were immediately followed by a 0V waiting period of 15s, 50s, 120s, and 300s, respectively. The zero of time for these latter curves corresponds to the end of the +0.28 volt filling pulse.

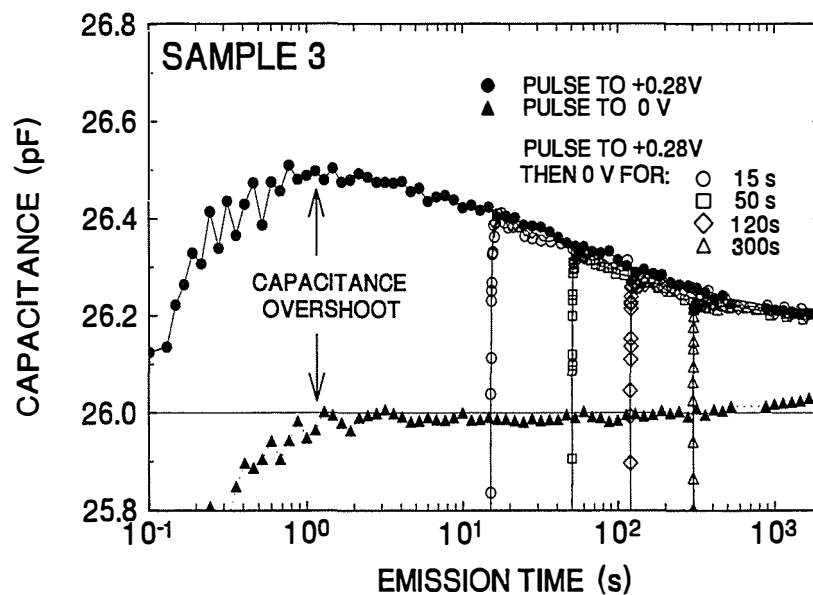
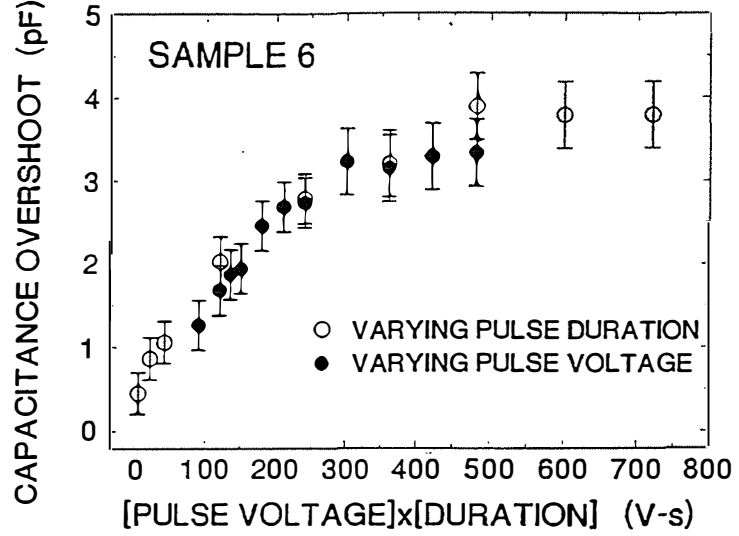


**FIG. 8.** Capacitance overshoot vs. the *product* of the filling pulse voltage ( $V_p$ ) and the filling pulse duration ( $t_p$ ) for sample 6 at 370 K. Pulse durations covered the range 10s to 1800s for a fixed 0.4V pulse voltage, and pulse voltages were varied between 0.3V to 1.6V for a fixed 300s pulse duration. The ambient reverse bias was -1.0 volts.



is zero or slightly *negative* (i.e. still in reverse bias), the long time, hole-emission type behavior is not observed. This suggests that hole injection from  $p^+$ -silicon is a necessary condition for the occurrence of this second type of transient. Also, the absence of the hole-emission type transients for the forward biased Schottky barrier contacts (samples 2 and 4), where no hole injection can occur, strongly supports this conclusion. We denote the *difference* between the peak capacitance during the transient and the pre-pulse capacitance as the “capacitance overshoot”.

Figure 8 plots the capacitance overshoot of sample 6 versus the *product* of the filling pulse voltage ( $V_p$ ) and the filling pulse duration ( $t_p$ ). We see that the overshoot increases until the  $V_p \times t_p$  product reaches a value of about 400 V-s and then saturates. Thus, the maximum number of states/traps that can be filled by the holes is well defined. This allows unambiguous comparisons between trap densities for different samples.

We can demonstrate that the capacitance overshoot transients are due to traps at the heterojunction interface. Beyond a few volts of reverse bias,  $V_b$ , the depletion region will extend through the a-Si:H layer and the a-Si:H/a-Si,Ge:H interface into the a-Si,Ge:H alloy. Hence, Poisson’s equation can be integrated to obtain [6]

$$V_b = \frac{1}{\epsilon} \int_0^d x \rho_{a-Si:H}(x) dx + \frac{Q_{int} d}{\epsilon} + \frac{1}{\epsilon} \int_d^W x \rho_{a-Si,Ge:H}(x) dx, \quad (4)$$

where  $\epsilon$  is the (average) dielectric constant,  $x$  is the distance from the barrier,  $\rho(x)$  is the charge density,  $d$  is the thickness of a-Si:H layer,  $W$  is the total depletion width (using the abrupt depletion approximation) and  $Q_{int}$  is the a-Si:H/a-Si,Ge:H interface charge density. After the filling pulse is removed the depletion width at time  $t$ ,  $W(t)$ , varies from its pre-pulse value,  $W_i$ . Since the bias voltage is restored to its pre-pulse value after the filling pulse, we have

$$\Delta V_b = 0 = \frac{1}{\varepsilon} \int_0^d x \Delta \rho_{\text{a-Si:H}}(x) dx + \frac{\Delta Q_{\text{int}}(t)d}{\varepsilon} + \frac{1}{\varepsilon} \int_d^{W(t)} x \rho_{\text{a-Si,Ge:H}}(x) dx - \frac{1}{\varepsilon} \int_d^{W_i} x \rho_{\text{a-Si,Ge:H}}(x) dx, \quad (5)$$

provided we neglect the charge emission within a-Si,Ge:H layer. This is reasonable in the long-time limit in which we observe these transients. If we further neglect the charge emission within the a-Si:H layer in this time regime, then the first integral vanishes and the interface charge

density can be written as

$$\Delta Q_{\text{int}}(t) = \frac{\varepsilon^2 A^2 \rho_{\text{a-Si,Ge:H}}^{\text{ave}}}{2d} \left[ \frac{1}{C_i^2} - \frac{1}{C(t)^2} \right], \quad (6)$$

where A is the active area,  $\rho_{\text{a-Si,Ge:H}}^{\text{ave}}$  is the average charge density in a-Si,Ge:H, and we have used the relations  $C_i \approx \frac{\varepsilon A}{W_i}$  and,  $C(t) \approx \frac{\varepsilon A}{W(t)}$ , for the initial capacitance and the capacitance at time t,

respectively. According to this analysis, if the capacitance transients are dominated by the emission of interface charge, then the right hand side of Eq. (6) should be independent of the applied bias provided it is large enough to allow complete depletion of the interface traps.

Figure 9(a) provides a comparison of the capacitance overshoots for sample 7 as a function of time for different values of the ambient bias under otherwise identical pulsing conditions. The calculated interface charge density from Eq. (6) corresponding to these transients is shown in Fig. 9(b). The value of  $\rho_{\text{a-Si,Ge:H}}^{\text{ave}}$  for each sample was obtained from drive-level capacitance profiling [7] within the a-Si,Ge:H layer (in this case  $\rho_{\text{a-Si,Ge:H}}^{\text{ave}} \approx 2 \times 10^{16} \text{ cm}^{-3}$ ). The close overlap of these curves indicates that the charge emission is indeed occurring from within a very localized spatial region.

A comparison of the interface charge densities for samples 5 and 6 obtained under saturation conditions is shown in Fig. 10. According to Table I, these two samples are identical except for the a-Si:H/a-Si,Ge:H interface treatment. From drive-level measurements, we find that the density of states for the a-Si,Ge:H layer in both samples 5 and 6 is nearly identical (about  $1.5 \times 10^{16} \text{ cm}^{-3}$ ) while their deduced trap densities are substantially different. Since the only difference between these two samples was their interface preparation, this verifies that the observed traps are located very close to the interface. In Table III we have listed the saturation values of the interfacial trap densities for the samples studied. For samples 1 and 3, the transients were not recorded under conditions of complete saturation, so the actual trap densities are probably larger than the values listed in the Table.

**FIG. 9. (a).** Capacitance transients for sample 7 using the same 1.6 volt, 300s filling pulse, but using different ambient bias voltages as indicated. **(b)** Calculated interface trap density derived using Eq. (6) for each transient in (a). The close overlap of these different curves confirms that the dominant traps are confined to a particular spatial location (the heterojunction interface).

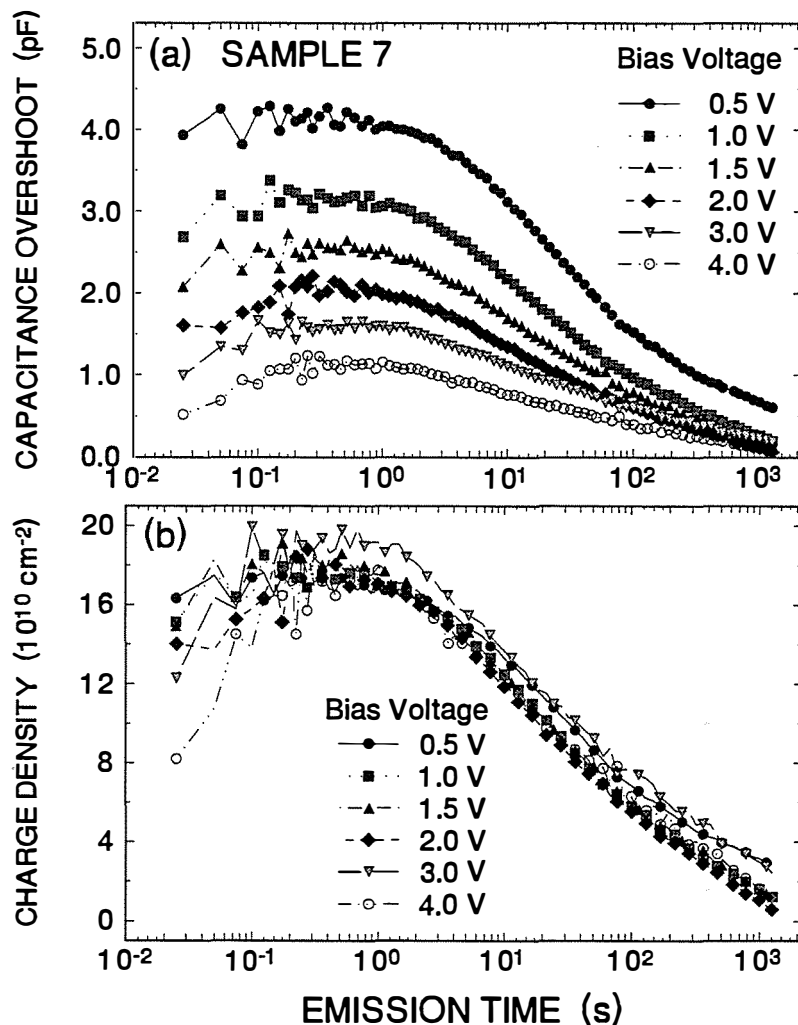


**FIG. 10.** Charge transients deduced from capacitance transient measurements on a-Si:H/a-Si,Ge:H heterojunction samples. The magnitude of the areal density of holes traps depends upon the type of interface preparation procedure that is employed.

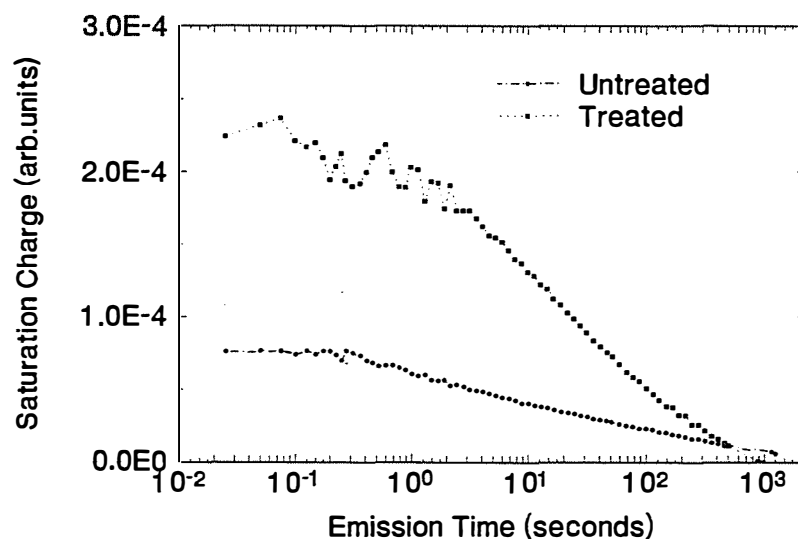


**TABLE III.** Summary of deduced interface trap densities for a-Si,Ge:H/a-Si:H samples.

#	Sample Configuration	Interface	$Q_{\text{int}}$ ( $\text{cm}^{-2}$ )
1	a-Si:H   a-Si,Ge:H	Untreated	$> 1 \times 10^{11}$
2	a-Si,Ge:H   a-Si:H	Untreated	Not observed
3	a-Si:H   a-Si,Ge:H	Untreated	$> 4 \times 10^{10}$
4	a-Si,Ge:H   a-Si:H	Untreated	Not observed
5	a-Si:H   a-Si,Ge:H	Untreated	$6 \times 10^{10}$
6	a-Si:H   a-Si,Ge:H	Treated	$1.6 \times 10^{11}$
7	a-Si:H   a-Si,Ge:H	Graded (250 Å)	$1.8 \times 10^{11}$
8	a-Si:H   a-Si,Ge:H	Graded (1000 Å)	$7 \times 10^{10}$

To examine the role of these traps in carrier recombination processes, we modified the timing sequence of the transients as follows: At the end of the filling pulse, the sample was held at zero bias for a certain period before the reverse bias was restored to produce the transients. This allowed an increased density of electrons to be present at the heterojunction interface. The transients recorded with these pulsing conditions for sample 3 are included in Fig. 7, where the time at zero bias has been added to the elapsed emission time. The excellent overlap of these curves indicates that the hole emission kinetics are not affected by the presence of the extra electrons. This means that the interface states are not acting as recombination centers for electrons. Also, because the charge emission continues in an identical manner in the absence of an electric field, this eliminates the possibility that the transients arise from polarization effects.

The transients for sample 8, in which the a-Si:H/a-Si,Ge:H interface was graded very gradually over 1000 Å, are qualitatively similar to the other samples. However, the capacitance at long times after the filling pulse does not return to its pre-pulse value even after raising the sample to higher temperature ( $\sim 420$  K). This suggests a metastable change in the state of the sample. If a subsequent filling pulse is applied, the resultant transient again indicates a trap density the same as for the prior transients. Since the only difference between sample 8 and sample 7 is the distance over which the interface is graded, this indicates that such metastable changes in the charge state of the traps result from the broader spatial extent of the interfacial region in sample 8. Also, in case of sample 8, the maximum number of traps that can be occupied and subsequently emptied is considerably smaller than that in sample 7 (See Table III).

While it is clear that the concentration of these traps is determined by the interface preparation during growth, we should also note that, in the deposition of all of these films, the plasma was interrupted between the a-Si:H layer and the a-Si,Ge:H layer. It is nonetheless more likely that these traps are inherent to the interface than a result of plasma interruption. Since the holes at these interface traps do not recombine with electrons, devices incorporating these interfaces may not be too adversely impeded. However, at levels of  $10^{11} \text{ cm}^{-2}$ , trapped interface charges will significantly alter the electric field profiles in such devices and thus affect the quantum efficiencies. Therefore, the control of these interfacial trapping states appears to be essential for device optimization.

## 6.0 PROPERTIES OF a-Si:H DEPOSITED WITH HYDROGEN OR HELIUM DILUTION

We have carried out comparison studies between a-Si:H samples grown by the glow discharge method either with 100% silane, or with silane diluted in  $\text{H}_2$  or He gas. The samples were obtained through collaboration with V. Perez-Mendez group at Lawrence Berkeley Laboratory [15], and further details concerning the growth conditions of these a-Si:H samples are given in Section 2.3. The purpose of this study is two-fold: First we wanted to evaluate the reliability of our capacitance characterization methods for n-i-p device structures by a direct comparison of results using such device structures with pure i-layer a-Si:H films deposited on doped crystalline Si with Pd Schottky contacts [denoted as  $\text{p}^+(\text{c-Si})\text{-i-m}$ , our usual sample configuration for capacitance measurements], and also with a-Si:H deposited on n+ a-Si:H on top of Cr coated glass with Schottky contacts at the top surface [n-i-m]. Second, we wanted to compare the electronic properties, particularly the stability properties, of hydrogen diluted, helium diluted, and undiluted glow discharge deposition.

Samples were characterized by drive-level capacitance profiling (DLCP) measurements as described in Section 3. An example of the profiles obtained for one  $\text{H}_2$  diluted n-i-p sample (Sample 1) at a series of measurement temperatures is shown in Fig. 11. Typically, a good estimate of the total deep defect density is obtained by doubling the profile value for the 100Hz, 400K case. Such an estimate has been found to agree quite well with ESR spin densities for a-Si:H samples.[5] For this sample, this implies a deep defect density of only  $9 \times 10^{14} \text{ cm}^{-3}$ . By the same method, the defect density for the standard sample (undiluted discharge) would be  $3 \times 10^{15} \text{ cm}^{-3}$ , which agrees quite well with previously measured high quality glow discharge samples.

Next, we repeated measurements on some samples using the n-i-m or the  $\text{p}^+(\text{c-Si})\text{-i-m}$  configurations. A couple examples of such comparisons are displayed in Fig. 12 where we have

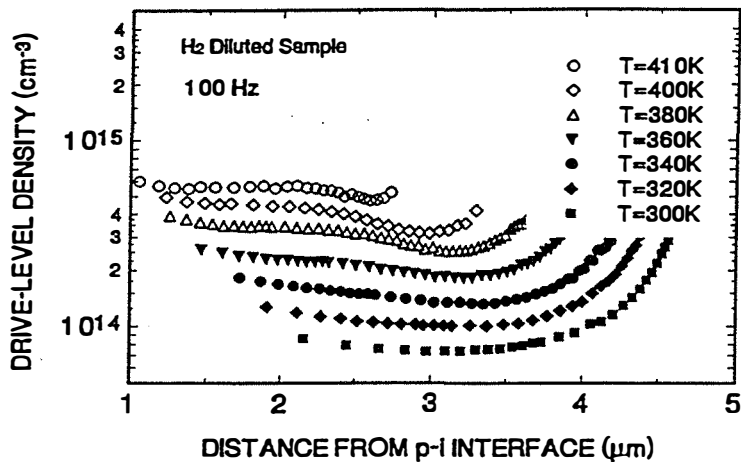


**FIG. 11** Example of 100Hz drive-level capacitance profiling data measured for a series of fixed temperatures for sample 1. A good estimate for the total deep defect density is obtained from doubling the drive-level density for the 400K profile.

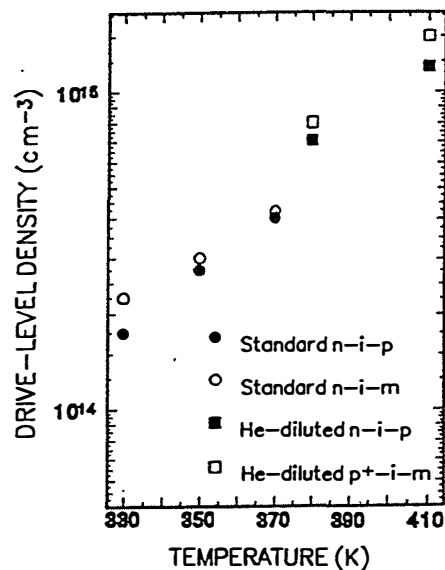


**FIG. 12.** Comparison of drive-level densities (spatially averaged) for different contacting configurations for two types of a-Si:H films.

plotted the spatially averaged DLCP values at several temperatures for two samples each with different contacting configurations. In all cases the DLCP values are *identical to within a factor of 1.25*, independent of the contacts. Thus the DLCP defect densities uniquely reflect the properties of the i-layer in each sample.

The electron and hole mobilities were determined for these samples at LBL using the standard time-of-flight (TOF) technique. A summary of the determined values for  $\mu_e$  and  $\mu_p$  are listed in Table IV in the annealed state along with the DLCP defect density estimate for each of the six samples. These DLCP measurements were carried out at 100Hz at a measurement temperature of 410K. This means that, according to Eqs. (2) and (3), the DLCP defect densities correspond to an integral from the bulk Fermi level to an energy of roughly 0.87eV below  $E_C$ . We see that the hydrogen diluted samples show improved transport properties for both electrons and holes and, correspondingly, a greatly reduced deep defect density when compared to either the He or standard glow discharge samples.

Finally, we compared the light-induced degradation of one hydrogen diluted sample (sample 1) with the standard sample (sample 6). Both samples were exposed for up to 300 hours to a 1.9eV red filtered tungsten-halogen light source at an intensity of 3.4 W/cm<sup>2</sup>. The samples were immersed in methanol during light soaking to maintain their surface temperatures below 65°C. We display the drive-level profiles obtained at a measurement temperature of 370K and a frequency of 10 Hz as a function of light exposure in Fig. 13. Here we see a substantially lower degraded defect density in the hydrogen diluted sample at each exposure, as well as much earlier

**TABLE IV.** Carrier mobilities and deep defect densities for samples in their dark annealed states. The TOF mobility measurements were carried out at LBL.

Sample	Dilutant Gas	$\mu_e$ ( $\text{cm}^2/\text{V}$ )	$\mu_h$ ( $\text{cm}^2/\text{V}$ )	$N_D$ ( $\text{cm}^{-3}$ )
1	H <sub>2</sub>	4.2	0.013	$9 \times 10^{14}$
2	H <sub>2</sub>	2.8	0.009	$1.0 \times 10^{15}$
3	H <sub>2</sub>	2.3	0.006	$9 \times 10^{14}$
4	He	1.2	0.003	$1.0 \times 10^{15}$
5	He	0.7	0.004	$2.2 \times 10^{15}$
6	none	1.0	0.004	$2.8 \times 10^{15}$

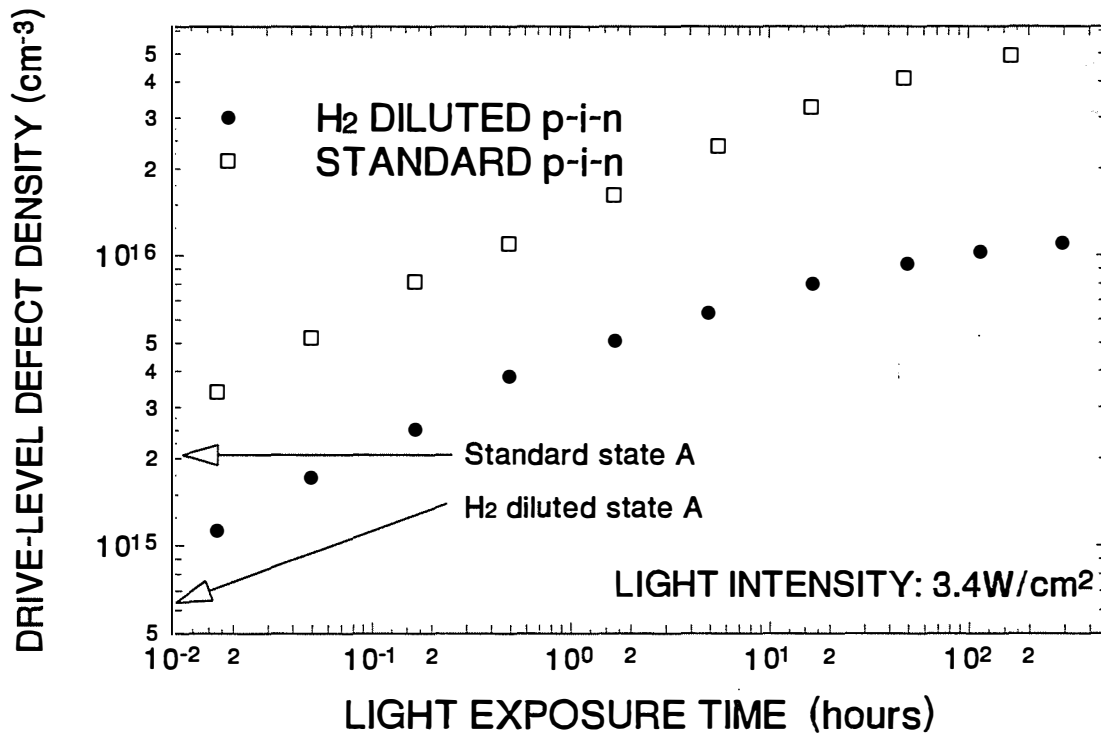


**FIG. 13.** Comparison of drive-level determined defect densities for sample 1 and sample 6 as a function of light exposure. The total defect densities are estimated by multiplying these drive-level values by a factor of 1.5.

saturation in that case. Ultimately, *the hydrogen diluted sample exhibits at least a factor of five improvement compared to the standard glow discharge a-Si:H sample.* Further measurements to test the degraded properties of the remaining samples are in progress.

## 7.0 SUMMARY AND CONCLUSIONS

The work carried out during this second phase of our NREL Subcontract has been focused on degradation studies in both pure a-Si:H and the a-Si,Ge:H alloys, as well as a detailed study of the interface between these two materials in a-Si:H/a-Si,Ge:H heterostructures. All samples discussed in this report were produced by the glow discharge method. The a-Si,Ge:H and heterostructure samples were obtained through an ongoing collaboration with United Solar Systems Corporation (J. Yang and S. Guha) while the a-Si:H samples, produced mostly under conditions of silane dilution, were obtained in collaboration with researchers at Lawrence Berkeley Laboratory (F. Zhong, W.S. Hong, and V. Perez-Mendez).

First of all, the results from our a-Si,Ge:H degradation studies represent a continuation of our attempts to fully understand the electronic properties of these alloys. The work completed during this phase represents our most focused effort to understand the light induced degradation in a-Si,Ge:H. Previously we had identified at least one type of defect band transition in these alloys that did not seem to be present in pure a-Si:H and had hypothesized that it could correspond to a significant population of  $D^+$  states in the nominally intrinsic a-Si,Ge:H alloy material. The light induced degradation studies seem to support this conclusion and, furthermore, indicate that charged defect ratios can vary significantly after light soaking. This undoubtedly will have important consequences for understanding the degradation process in a-Si,Ge:H devices. Additional studies are now underway to examine the properties of very lightly n- and p-type a-Si,Ge:H material, both to verify the assignments we have tentatively made to the different observed defect bands in this material, and also to obtain a more quantitative measure of the ratios of charged vs. neutral defects which are involved.

Second, we performed voltage pulse stimulated capacitance transient measurements on a-Si:H/a-Si,Ge:H heterostructure samples to look for carrier trapping states that might be associated with this interface. We found that, for filling pulses that put the interface into forward bias, there was a clear signature of trapped hole emission extending over long times. Furthermore, we were able to confirm that these hole traps were associated specifically with the interface itself in concentrations of roughly  $10^{11} \text{ cm}^{-2}$ . We found that treatment or grading of the interface modified the concentrations of these hole traps; however, they did not seem to act as recombination centers for electrons brought into the interface region. Nonetheless, these traps seem to exist in sufficient densities to significantly alter the electric field profiles across such

heterojunction structures and, therefore, they are likely to significantly impact the performance of tandem and triple cells which incorporate such interfaces.

Finally, we have begun a series of comparison studies of the electronic properties a-Si:H grown by glow discharge either with 100% silane, or with silane diluted in H<sub>2</sub> or He gas. These samples were predominantly n-i-p structures deposited on Cr coated glass, thus closely reproducing a popular photovoltaic device geometry, albeit with much thicker i-layers (at least 4 microns) to facilitate the capacitance profiling characterization method that we have used. The results on these samples indicate that the films grown under high hydrogen dilution exhibit roughly a factor of three lower deep defect densities than those grown using pure silane. Furthermore, in preliminary studies of light induced degradation in these samples, the hydrogen diluted samples degrade at a slower rate and saturate at a significantly lower value (by about a factor of five) than pure silane deposited sample. These results agree with reports of increased relative stability of cells employing hydrogen-diluted i-layers.[16,17] These studies are continuing to test the stability of the He diluted a-Si:H material, and plans to incorporate these types of alloys in modulated structures to try to understand the mechanisms for this increased stability are also being planned for Phase III.

## 8.0 SUBCONTRACT SUPPORTED PUBLICATIONS (1995-1996)

1. F. Zhong, C.-C. Chen, J.D. Cohen, P. Wickboldt, and W. Paul, "Defect properties of cathode deposited glow discharge amorphous silicon germanium alloys", *Mat. Res. Soc. Symp. Proc.* **377**, 553 (1995).
2. D. Kwon, J.D. Cohen, B.P. Nelson, and E. Iwaniczko, "Effect of light soaking on hot wire deposited a-Si:H films", *Mat. Res. Soc. Symp. Proc.* **377**, 301 (1995).
3. F. Zhong, C-C. Chen, and J.D. Cohen, "Electronic structure and light induced degradation of amorphous silicon-germanium alloys", *J. Non-Cryst. Solids*, **198-200**, 572 (1996).
4. Paul Wickboldt, Dawen Pang, William Paul, Joseph H. Chen, Fan Zhong, J. David Cohen, Yan Chen, and Don L. Williamson, "Improved a-Si<sub>1-x</sub>Ge<sub>x</sub>:H of large x deposited by PECVD", *J. Non-Cryst. Solids*, **198-200**, 567 (1996).
5. C. Palsule, J.D. Cohen, U. Paschen, "Capacitance characterization of amorphous silicon/amorphous silicon-germanium heterostructures", *Mat. Res. Soc. Symp. Proc.*, in press.
6. C-C. Chen, F. Zhong, J.D. Cohen, "Effects of light induced degradation on the distribution of deep defects in hydrogenated amorphous silicon-germanium alloys", *Mat. Res. Soc. Symp. Proc.*, in press.
7. F. Zhong, W.S. Hong, V. Perez-Mendez, C.-C. Chen, and J.D. Cohen, "The electronic properties of a-Si:H deposited with hydrogen or helium dilution", *Mat. Res. Soc. Symp. Proc.*, in press.

## 9.0 REFERENCES

- 1 . S. Guha, J.S. Payson, S.C. Agarwal, and S.R. Ovshinsky, *J. Non-Cryst. Solids* **97-98**, 1455 (1988).
- 2 . D.V. Lang, J.D. Cohen, and J.P. Harbison, *Phys. Rev.* **B25**, 5285 (1982).
- 3 . C.E. Michelson, A.V. Gelatos, and J.D. Cohen, *Appl. Phys. Lett.* **47**, 412 (1985).
- 4 . K.K. Mahavadi, K. Zellama, J.D. Cohen, and J.P. Harbison, *Phys. Rev.* **B35**, 7776 (1987).
- 5 . T. Unold, J. Hautala, and J.D. Cohen, *Phys. Rev.* **B50**, 16985 (1994).
- 6 . Lang, D.V. in Thermally Stimulated Relaxation in Solids, vol. 37 of Topics in Applied Physics, ed by P. Braunlich (Springer, Berlin, 1979), p. 93.
- 7 . Cohen, J.D., in Hydrogenated Amorphous Silicon, vol. 21C of Semiconductors and Semimetals, ed. by J. Pankove (Academic Press, New York, 1984), p. 9.
- 8 . J.D. Cohen and A.V. Gelatos, in *Advances in Disordered Semiconductors Vol I: Amorphous Silicon and Related Materials*, ed. by H. Fritzsche (World Scientific, Singapore, 1988), pp. 475-512.
- 9 . J. David Cohen, Thomas Unold, A.V. Gelatos, and C.M. Fortmann, *J. Non-Cryst. Solids* **141**, 142 (1992).
- 10 . T. Unold, J.D. Cohen, and C.M. Fortmann, *Mat. Res. Soc. Symp. Proc.* **258**, 499 (1992).
- 11 . A.V. Gelatos, K.K. Mahavadi, and J.D. Cohen, *Appl. Phys. Lett.* **53**, 403 (1988).
- 12 . J.D. Cohen, T. Unold, A.V. Gelatos, and C.M. Fortmann, *J. Non-Cryst. Solids* **141**, 142 (1992).
- 13 . F. Zhong, and J.D. Cohen, *Mat. Res. Soc. Symp. Proc.* **297**, 735 (1993).
- 14 . X.Xu, J. Yang, and S. Guha, *Appl. Phys. Lett.* **62**, 1399 (1993).
- 15 . Samples from Lawrence Berkeley Laboratory are courtesy of F. Zhong, W.S. Hong, and V. Perez-Mendez.
- 16 . Liyou Yang and Liang-Fan Chen, *Mat. Res. Soc. Symp. Proc.* **336**, 669 (1994).
- 17 . J. Yang, X. Xu, and S. Guha, *Mat. Res. Soc. Symp. Proc.* **336**, 687 (1994).

# REPORT DOCUMENTATION PAGE

*Form Approved*  
OMB NO. 0704-0188

Public reporting burden for this collection of information is estimated to average 1 hour per response, including the time for reviewing instructions, searching existing data sources, gathering and maintaining the data needed, and completing and reviewing the collection of information. Send comments regarding this burden estimate or any other aspect of this collection of information, including suggestions for reducing this burden, to Washington Headquarters Services, Directorate for Information Operations and Reports, 1215 Jefferson Davis Highway, Suite 1204, Arlington, VA 22202-4302, and to the Office of Management and Budget, Paperwork Reduction Project (0704-0188), Washington, DC 20503.

1. AGENCY USE ONLY (Leave blank)	2. REPORT DATE March 1997	3. REPORT TYPE AND DATES COVERED Annual Subcontract Report, 18 April 1995 - 17 April 1996	
4. TITLE AND SUBTITLE  Identifying Electronic Properties Relevant to Improving Stability in a-Si:H-Based Cells and Overall Performance in a-Si,Ge:H-Based Cells: Annual Subcontract Report, 18 April 1995 - 17 April 1996		5. FUNDING NUMBERS  C: XAN-4-13318-07 TA: PV704401	
6. AUTHOR(S)  J.D. Cohen		7. PERFORMING ORGANIZATION NAME(S) AND ADDRESS(ES)  Department of Physics and Materials Science Institute University of Oregon Eugene, Oregon	
8. PERFORMING ORGANIZATION REPORT NUMBER		9. SPONSORING/MONITORING AGENCY NAME(S) AND ADDRESS(ES)  National Renewable Energy Laboratory 1617 Cole Blvd. Golden, CO 80401-3393	
10. SPONSORING/MONITORING AGENCY REPORT NUMBER  SR-520-22701  DE97000225		11. SUPPLEMENTARY NOTES  NREL Technical Monitor: B. von Roedern	
12a. DISTRIBUTION/AVAILABILITY STATEMENT		12b. DISTRIBUTION CODE  UC-1262	
13. ABSTRACT ( <i>Maximum 200 words</i> )  The work done during this second phase of the University of Oregon's NREL subcontract focused on degradation studies in both pure a-Si:H and a-Si,Ge:H alloys, as well as a detailed study of the interface between these two materials in a-Si:H/a-Si,Ge:H heterostructures. All samples discussed in this report were produced by the glow-discharge method and were obtained either in collaboration with United Solar Systems Corporation or with researchers at Lawrence Berkeley Laboratory. First, the results from our a-Si,Ge:H degradation studies support the conclusion that considerable quantities of charged defects exist in nominally intrinsic material. Researchers found that on light-soaking, all the observed defect sub-bands increased; however, their ratios varied significantly. Second, researchers performed voltage pulse stimulated capacitance transient measurements on a-Si:H/a-Si,Ge:H heterostructure samples and found a clear signature of trapped hole emission extending over long times. Finally, researchers began comparison studies of the electronic properties of a-Si:H grown by glow discharge either with 100% silane, or with silane diluted in H <sub>2</sub> or He gas. The results on these samples indicate that the films grown under high hydrogen dilution exhibit roughly a factor of 3 lower deep defect densities than those grown using pure silane.			
14. SUBJECT TERMS  photovoltaics ; amorphous silicon ; amorphous silicon-germanium ; transient capacitance spectroscopy ; transient photocapacitance and photocurrent		15. NUMBER OF PAGES 32	
16. PRICE CODE		17. SECURITY CLASSIFICATION OF REPORT Unclassified	
18. SECURITY CLASSIFICATION OF THIS PAGE Unclassified		19. SECURITY CLASSIFICATION OF ABSTRACT Unclassified	
20. LIMITATION OF ABSTRACT  UL			